Peptidoglycan recycling mediated by an ABC transporter in the plant pathogen *Agrobacterium tumefaciens*

Michael C. Gilmore, Felipe Cava*

Laboratory for Molecular Infection Medicine Sweden (MIMS), Department of Molecular Biology, Umeå University, 90187 Umeå, Sweden

*For correspondence: felipe.cava@umu.se

Running title: Peptidoglycan recycling mediated by an ABC transporter

Keywords: bacterial cell wall, peptidoglycan recycling, *Agrobacterium tumefaciens*, Rhizobiales, ABC transporter

Abstract

During growth and division, the bacterial cell wall peptidoglycan (PG) is remodelled, resulting in the liberation of PG muropeptides which are typically reinternalized and recycled. Bacteria belonging to the Rhizobiales and Rhodobacterales orders of the Alphaproteobacteria lack the canonical muropeptide transporter AmpG, despite having other key PG recycling enzymes. Here, we show that an alternative transporter, YejBEF-YepA, takes over this role in the Rhizobiales phytopathogen *Agrobacterium tumefaciens*. Muropeptide import by YejBEF-YepA governs expression of the β-lactamase AmpC in *A. tumefaciens*, contributing to β-lactam resistance. However, we show that the absence of YejBEF-YepA causes severe cell wall defects that go far beyond lowered AmpC activity. Thus, contrary to previously established Gram-negative models, PG recycling is vital for cell wall integrity in *A. tumefaciens*. YepA is widespread in the Rhizobiales and Rhodobacterales, suggesting that YejBEF-YepA-mediated PG recycling could represent an important but overlooked aspect of cell wall biology in these bacteria.

Introduction

The bacterial cell wall is composed primarily of peptidoglycan (PG), a heteropolymer which consists of alternating *N*-acetylglucosamine (GlcNAc) and *N*-acetylmuramic acid (MurNAc) sugars crosslinked by short peptide chains (1). In order to facilitate growth and division, as well as adaption to environmental stressors, the cell wall is constantly remodelled by an arsenal of lytic enzymes (2): glucosaminidases and lysozyme cleave between the two sugars, endopeptidases cleave within the peptide chains, carboxypeptidases cleave the C-terminal amino acid from the peptide chains, amidases cleave the peptide chain from the MurNAc sugar and lytic transglycosylases (LTs) cleave between the sugars with simultaneous cyclisation of the terminal MurNAc to form 1,6-anhydroMurNAc. A consequence of this remodelling activity is the liberation of peptidoglycan fragments, termed muropeptides, which can be released into the environment where they can have far-reaching consequences in signalling or interspecies interactions (3), or imported into the cell for reuse in PG synthesis, in a process termed PG recycling (4).

PG recycling has been well studied in some Gram-negative models. Typically, anhydromuropeptides liberated by LTs are imported by the Major Facilitator Superfamily (MFS) transporter AmpG (5), before being broken into their constituent sugars and peptide by the amidase AmpD (6), β-hexosaminidase NagZ and LD-carboxypeptidase LdcA (7) (Fig. 1A). Pathways exist for recycling both the anhydroMurNAc and GlcNAc sugars (4, 8–10), while the peptide is directly reincorporated into PG synthesis by ligation with UDP-MurNAc by the ligase Mpl (11). Around 50% of the sacculus is turned over in *E. coli* per generation (12), but

only around 8% is released to the medium, due to recycling (13). Despite the extent of PG turnover, the abundance of proteins produced solely to enable PG recycling and its relatively wide conservation, its importance is unclear, since its interruption does not affect bacterial growth under laboratory conditions (4). The exception to this is a growth defect caused by the deletion of the LD-carboxypeptidase LdcA, which leads to a reduction in cell wall crosslinking due to the inability of tetrapeptide precursors to be used as a donor in the PG transpeptidation reaction (7, 14).

We noticed that Alphaproteobacteria belonging to the orders Rhizobiales and Rhodobacterales lack AmpG orthologs, despite encoding orthologs of other PG recycling enzymes such as AmpD and NagZ in their genomes. Using the plant pathogen *Agrobacterium tumefaciens* as model, we identified that the broad-specificity peptide ABC transporter YejBEF takes over the role of AmpG as muropeptide transporter in these bacteria, utilising an alternative PG-specific substrate-binding protein (SBP) YepA which is unique to the Alphaproteobacteria. PG recycling mediated by YejBEF-YepA governs expression of the β-lactamase AmpC through a canonical AmpR repression system, controlling β-lactam resistance in *A. tumefaciens* in place of AmpG. Importantly, we show that contrary to previously established Gram-negative models, PG recycling is vital for cell wall integrity in this bacterium since deleting the transporter results in significantly altered cell wall density and composition, leading to growth defects on low-osmolarity medium and hypersensitivity to β-lactam antibiotics in a manner partly independent of AmpC.

72 # Results

73 ## *A. tumefaciens* recycles PG

74 We first set out to determine if *A. tumefaciens* recycles PG, since it lacks an
75 ortholog of the PG recycling transporter AmpG. Since deletion of the
76 anhydromuramoyl-amidase AmpD results in the accumulation of
77 anhydromuramyltripeptides in the cytoplasm of *E. coli* (6), we deleted the *A.*
78 *tumefaciens* orthologs of both *ampD* (Atu2113) and *nagZ* (Atu1709) and used ultra-
79 performance liquid chromatography coupled to quadrupole-time of flight mass
80 spectrometry (UPLC-MS) to check for the accumulation of the substrates of these
81 enzymes in the cytoplasm (Fig. 1B). We observed the accumulation of
82 anhydroMurNAc- and MurNAc-linked muropeptide species accumulating in the
83 cytoplasm of Δ*ampD*, while the GlcNAc-anhydroMurNAc and GlcNAc-MurNAc
84 disaccharides accumulated in the cytoplasm of Δ*nagZ*, confirming these enzymes
85 play the same respective roles in PG recycling in *A. tumefaciens* as in other Gram-
86 negative bacteria. Interestingly, we observed tri-, tetra- and pentapeptide
87 muropeptides accumulating in Δ*ampD*. In *E. coli*, typically only tripeptide
88 muropeptides are observed to accumulate in an *ampD* mutant due to the activity of
89 the LD-carboxypeptidase LdcA (6), suggesting that *A. tumefaciens* lacks this activity
90 in its cytoplasm. To confirm this, we ectopically expressed LdcA from *E. coli* in *A.*
91 *tumefaciens* on a plasmid, and observed a corresponding shift in accumulation from
92 tetrapeptide to tripeptide muropeptides (Fig. S1). Additionally, trisaccharide
93 muropeptides also accumulated in Δ*ampD*, suggesting that *A. tumefaciens* can
94 transport dimers into its cytoplasm for recycling. The ion masses of these were
95 consistent with either crosslinked dimers or chains, but since LdcA expression
96 converted the di-tetrapeptide dimer into di-tripeptide (Fig. S1), they likely form chains

97 as the D-Ala is not crosslinked. Since *A. tumefaciens* does recycle PG, we reasoned
98 that it must have an alternative transporter of anhydromuropeptides.

99

100 Identification of the PG recycling transporter in *A. tumefaciens*

101 To identify the missing transporter, we took advantage of the antibiotic
102 Fosfomycin. This inhibits the first committed step of PG synthesis, the MurA-
103 catalysed conversion of UDP-GlcNAc into UDP-1-carboxyvinyl-GlcNAc, which forms
104 the substrate for the subsequent production of UDP-MurNAc by MurB (15). This step
105 can bypassed to some extent by the recycling of MurNAc, which confers higher
106 intrinsic resistance to Fosfomycin (8). We therefore used a high-throughput
107 transposon sequencing screen (Tn-Seq) to identify genes which are required for
108 survival under Fosfomycin treatment, reasoning that this should reveal genes
109 required for recycling MurNAc in *A. tumefaciens*, and thus our transporter. Our
110 Fosfomycin Tn-Seq screen revealed that recycling of MurNAc in *A. tumefaciens*
111 likely happens through the *Pseudomonas* pathway (8–10), using the enzymes AnmK
112 (Atu1827), MupP (Atu1614), AmgK (Atu0026) and MurU (Atu0025) to process
113 anhydroMurNAc and convert it into UDP-MurNAc for reuse (Supplementary Data 1).
114 In the list of genes which were statistically underrepresented in transposon insertions
115 with 2 mg/mL Fosfomycin (Fig. 2A, Supplementary Data 1), there were two ATP-
116 binding cassette (ABC) transporters. One consisted of the membrane-spanning and
117 nucleotide-binding proteins of the phosphonate ABC importer *phnJK*, which is
118 reported to form part of the carbon-phosphorus (C-P) lyase machinery (16, 17).
119 Since this complex mediates the cleavage of C-P bonds, such as that found in
120 Fosfomycin, it likely confers resistance to Fosfomycin by degrading it. Indeed,
121 degradation of Fosfomycin by Rhizobiales bacteria has been previously observed

122 (18), and this process could explain the relatively high intrinsic Fosfomycin
123 resistance in *A. tumefaciens*. The other ABC transporter with significantly reduced
124 Tn insertions was a putative peptide ABC importer previously reported as YejABEF
125 (Fig. 2A) consisting of two membrane-spanning proteins *yejB* and *yejE* (Atu0188 and
126 Atu0189) and an ATPase *yejF* (Atu0190). Interestingly, these genes form an operon
127 with a periplasmic substrate-binding protein (SBP), *yejA* (Atu0187) which was not
128 affected in Tn insertions under Fosfomycin treatment. Instead, our screen identified
129 an alternative peptide-binding SBP (Atu1774) with significantly fewer Tn insertions,
130 which showed sequence similarity to *yejA* (38.7% identity). The YejABEF ABC
131 transporter has previously been reported as a broad-specificity peptide importer
132 required for resistance to plant antimicrobial peptides and proper bacteroid
133 differentiation in *Sinorhizobium meliloti* (19, 20), and thus together with the SBP
134 Atu1774, represented a good candidate for an importer of muropeptides.

135 To investigate whether YejABEF constitutes a novel PG recycling transporter
136 in *A. tumefaciens*, we deleted the full operon corresponding to *yejABEF* (Atu0187-
137 Atu0190) (Fig. 2C) and used UPLC to check the supernatant of this mutant for the
138 accumulation of PG fragments. As would be expected, anhydromuramyl tri-, tetra-
139 and peptapeptides accumulated in large quantities in the extracellular milieu of the
140 Δ*yejABEF* mutant (Fig. 2B). Since deletion of *ampD* results in the accumulation of
141 muropeptides in the cytoplasm of *A. tumefaciens*, we reasoned that deletion of the
142 transporter in a Δ*ampD* background must necessarily prevent this. We therefore
143 checked the cytoplasmic soluble muropeptides in a Δ*yejABEF*Δ*ampD* mutant (Fig.
144 2D) using UPLC. There was no cytoplasmic muropeptide accumulation in the double
145 mutant, indicating that YejABEF is the sole transporter responsible for muropeptide
146 recycling in *A. tumefaciens*. Further, ectopic expression of the known MFS

147 muropeptide importer AmpG from *E. coli* restored the cytosolic accumulation of
148 muropeptides in the Δ*yejABEF*Δ*ampD* background (Fig. S2), confirming that these
149 transporters have the same function. Finally, we produced anhydro-disaccharide
150 tetrapeptides with the non-canonical D-amino acid D-Met instead of D-Ala in the
151 fourth position ($M4N^{Met}$) as a probe for PG recycling (14). Δ*ampD* cultures
152 exogenously supplemented with $M4N^{Met}$ yielded an accumulation of
153 anhydroMurNAc-$P4^{Met}$ (i.e., $M4N^{Met}$ processed by NagZ) in the cytoplasm (Fig. 2E),
154 which did not occur in the Δ*yejABEF*Δ*ampD* mutant, further confirming the
155 requirement of YejABEF for the import of anhydromuropeptides into the cytoplasm.

156

157 Role of PG recycling in β-lactam resistance in *A. tumefaciens*

158 *A. tumefaciens* encodes a canonical inducible AmpC β-lactamase system
159 where the import of anhydromuropeptides controls β-lactamase expression through
160 the regulator AmpR (21, 22)(Fig. 3A). We therefore reasoned that the Δ*yejABEF*
161 mutant could show decreased Amp resistance through lower β-lactamase
162 expression. Indeed, we observed a >250-fold decrease in Amp MIC in the
163 transporter mutant (Fig. 3B). Consistently, hydrolysis of the chromogenic
164 cephalosporin nitrocefin was decreased considerably in the mutant, indicating lower
165 AmpC activity (Fig. 3C).

166 Interestingly, the three parts of the transporter that are required for
167 Fosfomycin resistance form a cluster with the putative SBP YejA (Atu0187). Using
168 RT-PCR, we confirmed that *yejA* is co-expressed with *yejBEF* on a single mRNA
169 (Fig. S3A). As mentioned, Tn insertions in *yejA* were not significantly reduced under
170 Fosfomycin treatment. Instead, we found that mutation of the *yejA* paralog Atu1774

171 conferred Fosfomycin sensitivity. To investigate the potential role of these SBPs, we
172 generated single mutants of *yejA* and Atu1774 and compared them with mutants of
173 other parts of the transporter (Fig. 3C). The ampicillin sensitivity of the Δ*yejB*, Δ*yejE*,
174 Δ*yejF* and ΔAtu1774 mutants recapitulated that of the entire operon deletion mutant
175 (Fig. S3B), indicating that these components are required for the PG recycling
176 function of the transporter, while the Δ*yejA* mutant was phenotypically identical to the
177 WT. Additionally, we observed the accumulation of PG fragments in the supernatant
178 of ΔAtu1774 on the same levels as for Δ*yejABEF*, while Δ*yejA* again reflected the
179 WT (Fig. 3E). Collectively these results demonstrate that Atu1774, instead of YejA, is
180 the SBP involved in PG recycling in *A. tumefaciens*, and so we renamed it YepA for
181 Yej-peptidoglycan binding protein A.

182 Remarkably, we noticed that Δ*yejABEF* and the single mutants Δ*yejB,* Δ*yejE,*
183 Δ*yejF and* Δ*yepA* were more Amp sensitive than Δ*ampC* (Fig. 3B), meaning that the
184 Amp hypersensitivity of the PG recycling defective mutants was not just a result of
185 decreased β-lactamase activity. Indeed, the nitrocefin hydrolysis assay showed that
186 Δ*yejABEF* retained more β-lactamase activity than Δ*ampC* despite its lower Amp
187 resistance (Fig. 3C). This was further confirmed by testing sensitivity of both mutants
188 to aztreonam, a monobactam β-lactam antibiotic. The Δ*ampC* mutant showed an
189 identical resistance profile to the WT, suggesting that AmpC plays no role in
190 resistance of *A. tumefaciens* to aztreonam, while Δ*yejABEF* was once again
191 hypersensitive (Fig. 3F).

192

PG recycling is required for cell wall integrity in *A. tumefaciens*

We therefore hypothesised that the absence of YejBEF-YepA-mediated PG recycling might cause cell wall defects which result in increased sensitivity to β-lactam antibiotics. To challenge cell wall strength, we first grew PG recycling-defective mutant and WT strains in LB with no added NaCl (LB_0) to see how growth would be affected by low-osmolarity conditions. The Δ*yejB* mutant (phenotypically identical to the total Δ*yejABEF* mutant) displayed cell swelling and lysis (Fig. 4A), while the Δ*yejABEF* and Δ*yepA* mutants (but not Δ*yejA*) had a severe growth defect (Fig. 4B, S4A) which indicated a compromised cell wall. To investigate this further, we chemically analysed the cell wall of the Δ*yejB* mutant and WT using UPLC. While total crosslinking was slightly decreased in the mutant (Fig. 4C), interestingly, LD-crosslinking was more affected than DD-crosslinking, which was actually slightly higher relative to the WT. Since LD-transpeptidases are not affected by most β-lactam antibiotics (23), a higher dependence of the Δ*yejABEF* mutant on PBPs for PG crosslinking could be a possible contributing factor to its decreased β-lactam tolerance. Importantly, the total amount of PG in the mutant, as determined by the area under the whole chromatogram normalized to the optical density of the culture, was decreased considerably (Fig. 4D), suggesting that PG biogenesis was compromised. Quantification of the primary soluble cytoplasmic PG precursor UDP-muramylpentapeptide (UDP-M5) showed a corresponding decrease (Fig. 4E), indicating that PG recycling is an important source of material for PG synthesis in *A. tumefaciens*.

To further investigate the cell wall defects of Δ*yejABEF*, we used Tn-Seq to identify genes which confer greater or reduced fitness to the mutant when interrupted by Tn insertion (Fig. 4F, 4G, Supplementary Data 2). Consistent with the observed

218 defects of Δ*yejABEF* in PG synthesis and crosslinking, we found that synthetically
219 detrimental mutants included a putative LD-transpeptidase (Atu1615), bifunctional
220 PBP (Atu0931), DD-carboxypeptidase (Atu1499), and lytic transglycosylases MltB
221 (Atu3779), MltG (Atu1099) and RlpA (Atu1500), suggesting that additive effects
222 caused by the loss of these PG synthesis and remodelling proteins in combination
223 with PG recycling results in loss of fitness or non-viability. These results were
224 recapitulated by a second Tn-Seq comparing insertions in the Δ*yepA* and Δ*yejA*
225 mutants (Fig. S4B).

226 Conversely, mutations in several glycosyltransferases (Atu2583, Atu2590,
227 Atu2592), a UDP-GlcNAc dehydrogenase (Atu2582) and a putative ABC exporter
228 (Atu2577) improved fitness of the Δ*yejABEF* mutant. These genes form part of a
229 cluster likely to be involved in the synthesis of an uncharacterized glycan, previously
230 reported to be required for resistance to phenazines in *A. tumefaciens* (24). Since its
231 synthesis seems to use UDP-GlcNAc as a building block, we hypothesized that
232 these mutations might redirect GlcNAc flux to PG synthesis, thereby improving
233 Δ*yejABEF* fitness. However, this does not seem to be the case, as measured UDP-
234 M5 and UDP-MurNAc levels in ΔAtu2582 and ΔAtu2582Δ*yejABEF* strains showed
235 no differences to their WT and Δ*yejABEF* counterparts (Fig. S4C). It remains to be
236 seen what role this polymer plays in cell wall biology in *A. tumefaciens*.

237

238 YejBEF-YepA is conserved in the Rhizobiales and Rhodobacterales
239 orders of the Alphaproteobacteria

240 Finally, to define the degree of conservation of the PG recycling function of
241 YejBEF in bacteria, we generated a molecular fingerprint that allowed us to

242 differentiate between YepA and YejA. Using the JDet package (25), we generated a
243 set of specificity-determining residues from an alignment of YejA and YepA orthologs
244 (Fig. 5B). While YejABEF is broadly conserved across the proteobacteria, YepA is
245 exclusive to the Alphaproteobacteria (Fig. 5A), being present in almost all families in
246 the Rhizobiales and Rhodobacterales orders, which also mostly lack AmpG. These
247 bacteria inhabit a broad spectrum of niches including plant symbionts and pathogens
248 (Rhizobiales), mammalian pathogens (Brucellaceae, Bartonellaceae), soil bacteria
249 (Azospirilliceae) and photosynthetic marine bacteria (Rhodobacteriaceae)
250 suggesting that YejBEF-YepA is not associated with one particular lifestyle.
251 Interestingly, while most species opt either for AmpG or YejBEF-YepA, these PG
252 transporters seem to coexist in a number of species such as in the
253 Bradyrhizobiaceae indicating that one or both could be used under different
254 conditions.

255

256 Discussion

257 PG biosynthesis and remodelling have been the subject of decades of research, but
258 the focus on relatively few model organisms has left the diversity of these processes
259 poorly understood. This particularly applies to PG recycling, which has additionally
260 suffered from a perceived lack of importance, since its interruption in the Gram-
261 negative model organism *E. coli* has no detrimental effect to the bacterium under lab
262 conditions (4). Muropeptides are a unique molecular signature of bacteria which are
263 highly immunogenic (26) and often mediate interspecies interactions (3). Therefore,
264 PG recycling is a factor which influences bacterial virulence and immune response
265 activation (27–29). Additionally, the high turnover of PG during the cell cycle means

266 that significant amounts of material would be lost if it were not recycled. Many
267 bacteria outside the typical models lack orthologs of key PG recycling enzymes, but
268 have others (4), suggesting there are alternative enzymes or pathways to be
269 discovered. For example, it was recently uncovered that both *Vibrio cholerae* (14)
270 and *Acinetobacter baumanii* (30, 31) have different functional analogs of the *E. coli*
271 LD-carboxypeptidase LdcA with a separate but convergent evolution. We noticed
272 that many bacteria belonging to the Rhizobiales and Rhodobacterales orders of the
273 Alphaproteobacteria lacked an AmpG transporter despite having orthologs of the
274 other key PG recycling enzymes AmpD and NagZ. Using the plant pathogen *A.*
275 *tumefaciens* as model, we identified an alternative ABC transporter that takes over
276 this role. *A. tumefaciens* is a fascinating model to study the growth and division of
277 bacteria, because it exhibits an unusual asymmetric polar growth mode, and relies
278 heavily on the typically dispensable LD-transpeptidases for peptidoglycan
279 crosslinking (32).

280 What happens to the PG after it is transported into the cell? An interesting
281 difference between muropeptide recycling in *A. tumefaciens* and *E. coli* is the variety
282 of intracellular muropeptide species which accumulate in the Δ*ampD* mutant. In *E.*
283 *coli*, only the NagZ- and LdcA-processed anhydromuramyl tripeptide accumulates on
284 significant levels (5), whereas in our *A. tumefaciens* Δ*ampD* mutant, peaks
285 corresponding to a wide variety of anhydromuramyl tri-, tetra- and pentapeptides are
286 present as well as dimeric muropeptides (Fig. 1B). Since direct recycling of
287 tetrapeptide precursors is typically highly toxic to the cell (7, 14), and we were unable
288 to detect UDP-M4^{Met} on treating *A. tumefaciens* with M4N^{Met} (Fig. 2E), we suggest
289 that *A. tumefaciens* does not directly reuse the PG peptide by ligation with UDP-
290 MurNAc as in some other Gram-negative bacteria. Instead, it might simply degrade

291 the released peptides and reincorporate the released amino acids into *de novo*
292 precursor synthesis or use them as a source of C or N. This idea is supported by the
293 lack of Mpl ligase or LD-carboxypeptidase orthologs in *A. tumefaciens*, and by the
294 genetic context of *yejABEF* since it clusters with a putative D-alanine dehydrogenase
295 *dadA* (Atu0192, labelled as a pseudogene due to a frameshift mutation, but this
296 occurs after the catalytic domain suggesting that it could have retained its activity)
297 and glutamine synthetase *glnA* (Atu0193) which uses glutamate as a substrate.

298 It is interesting that the PG SBP YepA is located separately from the rest of
299 the transporter in the genome. This raises the possibility of separate transcriptional
300 regulation of the "core" and PG-binding parts of the transporter, which would allow its
301 PG recycling function to be regulated independently of its function as a broad-
302 spectrum peptide importer. Additionally, the presence of two SBPs competing for the
303 same core could allow regulation of transporter function at the protein level, since
304 higher levels of one SBP might be expected to preclude binding of the other. YepA
305 also seems to have a conserved position beside a both a predicted cytoplasmic
306 DsbA-like protein (Atu1775) of unknown function and the essential periplasmic polar
307 growth protein RgsG (33), but the function of these two genes remains to be
308 identified.

309 The presence of an AmpC induction system based on released muropeptides
310 has been previously reported in *A. tumefaciens* (21), but the mechanism through
311 which muropeptides enter the cell has not been revealed until now. As a soil
312 bacterium, *A. tumefaciens* likely encounters β-lactam antibiotics in the environment,
313 so the presence of an inducible β-lactamase system could be a way to counter
314 these. However, although YejBEF-YepA does control the induction of AmpC, we
315 showed that its effect on β-lactam sensitivity is also partly caused by cell wall defects

316 which occur in its absence. The requirement of PG recycling for cell wall integrity and
317 normal growth was surprising, since *E. coli* has been shown to have no physiological
318 defects on deletion of AmpG (4). Our Tn-Seq screen in Δ*yejABEF* revealed
319 synthetically lethal cell wall-related genes including a bifunctional PBP, an LD-
320 transpeptidase, and three LTs. Insertions in the synthetic PBP and LD-
321 transpeptidase could result in lethality due to additive effects on top of the synthesis
322 defects that already occur. Mutation of LTs is known to cause periplasmic stress due
323 to periplasmic crowding caused by the accumulation of PG chains (34). Interruption
324 of PG recycling could exacerbate periplasmic crowding, since we observed PG
325 fragments accumulating in large amounts in the supernatant of Δ*yejABEF*. That we
326 observe chains accumulating in the cytoplasm of Δ*ampD* but not in the supernatant
327 of Δ*yejABEF* suggests they could be too large to escape the outer membrane,
328 accumulating in the periplasm and thereby causing osmotic stress.

329 Our Tn-Seq screen also revealed that Tn insertions in a gene cluster likely
330 responsible for the synthesis of an uncharacterised glycan alleviated the fitness cost
331 of deleting Δ*yejABEF*. While this could be consistent with the idea of alleviating
332 periplasmic crowding, *A. tumefaciens* also produces osmoregulated cyclic β-glucans
333 (35), which did not show up in our screen, meaning this is likely not the case. This
334 polymer has previously been reported as required for tolerance of the phenazine
335 pyocyanin in *A. tumefaciens* (24), suggesting it could play some role in oxidative
336 stress metabolism. Cell wall defects have previously been associated with an
337 overproduction of hydroxyl radicals (36), and the potential role of YejBEF-YepA in
338 periplasmic oxidative stress is a subject for future research.

339 YejABEF has previously been reported as important for proper bacteroid
340 differentiation and resistance to the plant antimicrobial peptide NCR247 in *S. meliloti*

341 (20, 37). Though this was thought to be due to its activity as a promiscuous peptide
342 importer, we suggest that it actually comes from its function as a PG transporter,
343 since AmpD is also required for NCR247 tolerance and the non-PG SBP YejA is not
344 (37). Indeed, the bacteroids formed by *S. meliloti* Δ*yejE* and Δ*yejF* mutants (20)
345 share strikingly similar aberrant morphologies with our Δ*yejABEF* mutant grown on
346 low osmolarity medium (LB_0, Fig. 4A) indicating that PG recycling is necessary to
347 maintain cell wall integrity in *S. meliloti* during bacteroid differentiation. *A.*
348 *tumefaciens*, along with *Brucella abortus* and *Bartonella henselae*, is an intracellular
349 pathogen, and so "hiding" its released PG from the host could be an essential
350 strategy to avoid immune detection particularly since immune receptors for PG are
351 located intracellularly. The effect of the transporter on virulence and immune
352 response evasion in other related species remains to be studied, but the widespread
353 presence of YepA in the Alphaproteobacteria and its physiological importance to *A.*
354 *tumefaciens* suggests that PG recycling could be an important and overlooked
355 aspect of cell wall biology in these bacteria.

356 The question of why *A. tumefaciens* uses an ABC transporter to recycle PG
357 instead of a PMF-dependent MFS transporter such as AmpG remains. The use of
358 different energy sources could mean that PG recycling is required by *A. tumefaciens*
359 under a specific condition where ATP is available as an energy source but
360 membrane polarisation is affected. However, *yepA* does not seem to be limited to
361 any one particular niche, being present in diverse plant and animal pathogens and
362 symbionts also environmental and marine bacteria (Fig. 5). The Rhizobiales are
363 known to be particularly rich in ABC transporters, with 146 full ABC importers
364 present in *Sinorhizobium meliloti* (38, 39). One possible reason for this is that it could
365 facilitate a common mechanism of regulation of transport. Inactivation of ABC

366 transporters on a cellular scale has been identified previously in *Rhizobium*
367 *leguminosarum* in response to sensing of global cellular nitrogen availability (40–42)
368 or glutathione levels (43), through a putatively post-translational mechanism which
369 remains to be elucidated (40, 42). Therefore, using an ABC transporter for PG
370 recycling could allow the cell to coordinate the regulation of this process with the
371 regulation of acquisition of other nutrients and energy sources, perhaps in
372 synchronisation with the cell cycle since glutathione levels are known to fluctuate
373 during the cell cycle in the related Alphaproteobacterium *Caulobacter crescentus*
374 (44).

375

376 Methods

377 Strains and Growth Conditions

378 Strains used in this study are listed in Table S1. *A. tumefaciens* strains were
379 grown in LB, ATGN or ATSN (prepared as ref. (45) but without the addition of $FeSO_4$
380 to avoid precipitation as its absence did not affect growth) at 30°C unless stated
381 otherwise. *E. coli* strains were grown in LB at 37°C. All *A. tumefaciens* mutants are
382 derivatives of the *Agrobacterium fabrum* strain C58. When required, antibiotics were
383 added to growth media: Kanamycin (50 µg/mL *E. coli*, 300 µg/mL *A. tumefaciens*),
384 Ampicillin (100 µg/mL) or Chloramphenicol (20 µg/mL). Growth curves were done
385 using a microplate reader (Eon Biotek) to measure OD_{600} of 200 µL cultures in a 96-
386 well microplate over 28h at 5 minute intervals. Three technical replicates of three
387 biological replicates (i.e. separate parental cultures) were used per condition. Initial
388 cultures were prepared by adjusting exponentially growing cultures to OD_{600} 0.01.

389

390 ## Construction of Plasmids and Mutants

391 Expression and allelic exchange vectors were constructed using the primers
392 outlined in Table S2. Allelic exchange vectors for *A. tumefaciens* were constructed
393 using isothermal assembly of flanking regions with the suicide vector pNPTS139;
394 mutagenesis was carried out as described (46). Protein expression vectors were
395 constructed by PCR of the region of interest with addition of restriction sites by
396 primers, then restriction digest and ligation before transformation into *E. coli* DH5α.

397

398 ## Antibiotic Resistance Determination

399 Resistance to various antibiotics was determined on agar using MIC Test
400 Strips (Liofilchem). Exponential cultures were adjusted to OD_{600} 0.1 in PBS before
401 being spread across an LB agar plate three times using a sterile cotton swab; the
402 plate was rotated 60° between each spreading. The strip was applied once the plate
403 had dried fully.

404

405 ## Nitrocefin Hydrolysis Assay

406 Overnight cultures of *A. tumefaciens* strains were diluted 1:3 in fresh LB with
407 50 µg/mL ampicillin added (to induce *ampC* expression) and grown for 1 h. 1 mL of
408 culture normalised to OD_{600} 0.4 was prepared which was pelleted and washed in 1
409 mL of PBS. The final pellet was then resuspended in 1 mL lysis buffer (PBS with
410 0.2% Triton X-100, 50 µg/mL lysozyme and 2 mM EDTA) and incubated on ice for 30
411 min to lyse the cells. 200 µL reactions were set up containing 100 µL lysate, 96 µL
412 PBS and 4 µL 500 µg/mL nitrocefin (Oxoid) and the reaction was followed by
413 monitoring A_{486} for 2 h in a microplate reader (Eon Biotek) with readings every 5 min.

414

415 ## Soluble muropeptide and PG precursor analysis

416 To determine the presence and levels of intra- and extracellular soluble
417 muropeptides and precursors, bacteria were grown until late exponential phase
418 (roughly OD600 0.7) in minimal media before being cooled on ice for 10 min and
419 normalised to the same OD_{600}. Cells were then harvested by centrifugation at 10,000
420 × g for 2 min. The supernatant was decanted and passed through a 0.22 µm filter,
421 then boiled for 10 min, centrifuged at maximum speed in a benchtop centrifuge for
422 10 min to remove precipitated proteins and concentrated 20 times in a SpeedVac
423 system. Meanwhile, the cell pellet was washed three times in ice-cold 0.9% NaCl,
424 resuspended in 0.9% NaCl so that the cells are 20 times concentrated and boiled for
425 10 minutes before centrifugation at maximum speed in a benchtop centrifuge for 10
426 min to remove the proteins and insoluble fraction.

427 Detection and chemical characterisation of the soluble muropeptides was
428 carried out using an Acquity H-Class UPLC (Waters) coupled to a Xevo G2/XS
429 QTOF mass spectrometer. Chromatographic separation was achieved using an
430 Acquity UPLC BEH C18 column (Waters) maintained at 45°C. A linear gradient of
431 0.1% formic acid in water to 0.1% formic acid in acetonitrile was used for elution. UV
432 detection was performed at 204 nm. The QTOF instrument was operated in positive
433 ion mode, with data collection performed in untargeted MS^e mode. The parameters
434 were set as follows: capillary voltage 3.0 kV, source temperature 120°C, desolvation
435 temperature 350°C, sample cone voltage 40 V, cone gas flow 100 L h^{-1} and
436 desolvation gas flow 500 L h^{-1}. Data acquisition and processing was performed using
437 the UNIFI software (Waters). A compound library of expected muropeptides was built
438 in UNIFI by drawing the structures in ChemSketch (http://www.acdlabs.com). This

439 library was used for automated processing of the data and quantification by
440 integration of the peaks from extracted ion chromatograms.
441

442 Peptidoglycan Analysis

443 Peptidoglycan isolation and analysis were carried out as described previously
444 (47). Briefly, 10 mL stationary phase cultures were normalised to the same OD_{600},
445 pelleted, resuspended in 5% SDS and boiled for 2 h with stirring. The obtained
446 sacculi were washed repeatedly in water to remove the SDS before analysis;
447 pelleting was performed by ultracentrifugation in an Optima MAX-TL benchtop
448 ultracentrifuge at 150,000 x g. The final pellet was resuspended in water and
449 digested overnight with muramidase (80 µg/mL) before adjustment to pH 9.5 with
450 addition of 0.5 M sodium borate, reduction with addition of 10 mg/mL sodium
451 borohydride for 20 min at RT and adjustment to pH 3.5 by addition of
452 orthophosphoric acid.

453 Liquid chromatography was carried out using an Acquity H-Class UPLC
454 system (Waters) equipped with an Acquity UPLC BEH C18 column (2.1mm x 150
455 mm, 130 Å pore size and 1.7 µm particle size, Waters). Chromatographic separation
456 was achieved using a linear gradient from 0.1% formic acid in water to 0.1% formic
457 acid in acetonitrile. Peaks were identified by running a reference sample in LC-MS
458 using the same method as above and assigning peak identities using retention time.
459 The relative amount of each muropeptide was calculated by integrating all the peaks
460 and dividing each peak area by the total area of the chromatogram, while the total
461 area of the chromatogram was taken as the relative density of PG per sample and
462 expressed relative to the WT.

463

464 M4N^{Met} incorporation experiment

465 M4N was prepared by digesting purified *V. cholerae* sacculi using the lytic
466 transglycosylase MltA. An in vitro Ldt-mediated exchange reaction with purified LdtA
467 was used to swap the D-Ala in position 4 with D-Met to produce M4N^{Met} as described
468 (48). 10 mL of exponentially growing *A. tumefaciens* cultures was pelleted and
469 resuspended in 200 µL fresh medium, and approximately 15 µg M4N^{Met} was added
470 to each. The cultures were then grown for a further hour and prepared for soluble
471 precursor analysis as described above.

472

473 Bioinformatic Analyses

474 Sequences of SBPs corresponding to YejA and YepA were identified in
475 representative species spanning the Rhizobiales and Rhodobacterales orders of the
476 Alphaproteobacteria: *A. tumefaciens*, *Sinorhizobium meliloti*, *Bartonella henselae*,
477 *Brucella melitensis*, *Ochrobactrum anthropi*, *Dinoroseobacter shibae* and
478 *Phaeobacter inhibens*. SBPs were identified by phenotype for *D. shibae* and *P.*
479 *inhibens* (using FitnessBrowser (49) to look for the SBP with the expected β-lactam
480 and Fosfomycin sensitivity phenotypes) and eggNOG 5.0 (50) using fine-grained
481 orthologs of Atu1774 and Atu0187 for the others. Sequences were aligned using
482 MUSCLE (51) and the JDet package (25) was used to find specificity-determining
483 positions (SDPs), which were visualised using WebLogo (52). To produce a
484 phylogenetic tree, all YejA orthologs were downloaded from OrthoDB (53), aligned
485 using MUSCLE v5 and the previously determined SDPs were used to label each as
486 either YejA or YepA. AmpG orthologs from OrthoDB were filtered by BLASTP

487 against *E. coli* AmpG using an E value cutoff of $1x10^{-25}$. PhyloT was used to produce
488 a phylogenetic tree of all species on OrthoDB and orthologs of YejA, YepA and
489 AmpG were mapped against this. The final tree was visualised using iTOL (54).

490

491 RT-PCR of *yejABEF* cluster

492 All kits were used as per the manufacturer's instructions. Total RNA was
493 extracted from *A. tumefaciens* C58 WT using the RNeasy Plus Mini Kit (QIAGEN),
494 DNA was degraded using the TURBO DNA-free kit (Thermo) and cDNA was
495 synthesised using the Maxima Reverse Transcriptase (Thermo). PCR was
496 performed with primers FCP6349-6357 using the VeriFi polymerase (PCRBIO), with
497 a 64 °C annealing temperature and 1.5 min elongation time.

498

499 Transposon Sequencing

500 For identification of conditionally essential genes, transposon sequencing (Tn-
501 Seq) was performed broadly as described elsewhere (55), adapted for *A.*
502 *tumefaciens*. $3\text{-}5x10^5$ transposon mutants were generated per library by conjugation
503 of *A. tumefaciens* C58 with *E. coli* SM10λ-pir carrying the mariner transposon donor
504 plasmid pSC189 (56). Mutant libraries were selected on LB plates with 500 µg/mL
505 kanamycin (to select for the transposon), 25 µg/mL streptomycin (to remove the
506 donor *E. coli*) and 2 mg/mL Fosfomycin where appropriate. The libraries were
507 collected, genomic DNA extracted, and pooled genomic DNA fragments were
508 sequenced using a MiSeq system (Illumina). Insertion sites were identified and
509 statistical representation of transposon insertions determined using the ConArtist
510 pipeline as described (57).

Acknowledgements

We thank all members of the Cava lab for helpful comments and suggestions. Research in the Cava lab is supported by the Swedish Research Council, the Laboratory for Molecular Infection Medicine Sweden (MIMS), Umeå University, the Knut and Alice Wallenberg Foundation (KAW) and the Kempe Foundation.

References

1. W. Vollmer, D. Blanot, M. A. De Pedro, Peptidoglycan structure and architecture. *FEMS Microbiology Reviews* **32**, 149–167 (2008).

2. W. Vollmer, B. Joris, P. Charlier, S. Foster, Bacterial peptidoglycan (murein) hydrolases. *FEMS Microbiology Reviews* **32**, 259–286 (2008).

3. O. Irazoki, S. B. Hernandez, F. Cava, Peptidoglycan muropeptides: Release, perception, and functions as signaling molecules. *Frontiers in Microbiology* **10** (2019).

4. J. T. Park, T. Uehara, How Bacteria Consume Their Own Exoskeletons (Turnover and Recycling of Cell Wall Peptidoglycan). *Microbiology and Molecular Biology Reviews* **72**, 211–227 (2008).

5. C. Jacobs, L. J. Huang, E. Bartowsky, S. Normark, J. T. Park, Bacterial cell wall recycling provides cytosolic muropeptides as effectors for β-lactamase induction. *EMBO Journal* **13**, 4684–4694 (1994).

6. C. Jacobs, *et al.*, AmpD, essential for both β-lactamase regulation and cell wall recycling, is a novel cytosolic N-acetylmuramyl-L-alanine amidase. *Molecular Microbiology* **15**, 553–559 (1995).

7. M. F. Templin, A. Ursinus, J. V. Höltje, A defect in cell wall recycling triggers autolysis during the stationary growth phase of Escherichia coli. *EMBO Journal* **18**, 4108–4117 (1999).

8. J. Gisin, A. Schneider, B. Nägele, M. Borisova, C. Mayer, A cell wall recycling shortcut that bypasses peptidoglycan de novo biosynthesis. *Nature Chemical Biology* **9**, 491–493 (2013).

9. M. Borisova, J. Gisin, C. Mayer, The N-Acetylmuramic Acid 6-Phosphate Phosphatase MupP Completes the Pseudomonas Peptidoglycan Recycling Pathway Leading to Intrinsic Fosfomycin Resistance. *mBio* **8**, e00092-17 (2017).

10. C. Fumeaux, T. G. Bernhardt, Identification of MupP as a new peptidoglycan recycling factor and antibiotic resistance determinant in pseudomonas aeruginosa. *mBio* **8**, 1–13 (2017).

11. D. Mengin-Lecreulx, J. Van Heijenoort, J. T. Park, Identification of the mpl gene encoding UDP-N-acetylmuramate: L-alanyl- γ-D-glutamyl-meso-diaminopimelate ligase in Escherichia coli and its role in recycling of cell wall peptidoglycan. *Journal of Bacteriology* **178**, 5347–5352 (1996).

12. E. W. Goodell, Recycling of murein by Escherichia coli. *Journal of Bacteriology* **163**, 305–310 (1985).

13. E. Goodell, U. Schwarz, Release of Cell Wall Peptides into Culture Medium by Exponentially Growing Escherichia coli. *Journal of Bacteriology* **162**, 391–397 (1985).

14. S. B. Hernández, T. Dörr, M. K. Waldor, F. Cava, Modulation of Peptidoglycan Synthesis by Recycled Cell Wall Tetrapeptides. *Cell Reports* **31** (2020).

15. F. M. Kahan, J. S. Kahan, P. J. Cassidy, H. Kropp, The Mechanism of Action of Fosfomycin (Phosphonomycin). *Annals of the New York Academy of Sciences* **235**, 364–386 (1974).

16. P. Seweryn, *et al.*, Structural insights into the bacterial carbon-phosphorus lyase machinery. *Nature* **525**, 68–72 (2015).

17. A. K. White, W. W. Metcalf, Microbial metabolism of reduced phosphorus compounds. *Annual Review of Microbiology* **61**, 379–400 (2007).

18. J. W. McGrath, F. Hammerschmidt, J. P. Quinn, Biodegradation of phosphonomycin by Rhizobium huakuii PMY1. *Applied and Environmental Microbiology* **64**, 356–358 (1998).

19. M. Novikova, *et al.*, The Escherichia coli Yej transporter is required for the uptake of translation inhibitor microcin C. *Journal of Bacteriology* **189**, 8361–8365 (2007).

20. Q. Nicoud, *et al.*, Sinorhizobium meliloti Functions Required for Resistance to Antimicrobial NCR Peptides and Bacteroid Differentiation. *mBio* **12**, e00895-21 (2021).

21. W. M. Figueroa-Cuilan, *et al.*, Induction of AmpC-Mediated β-Lactam Resistance Requires a Single Lytic Transglycosylase in Agrobacterium tumefaciens. *Appl Environ Microbiol*, e0033322 (2022).

22. C. Jacobs, J.-M. Frère, S. Normark, Cytosolic Intermediates for Cell Wall Biosynthesis and Degradation Control Inducible β-Lactam Resistance in Gram-Negative Bacteria. *Cell* **88**, 823–832 (1997).

23. A. Aliashkevich, F. Cava, LD-transpeptidases: the great unknown among the peptidoglycan cross-linkers. *FEBS Journal* (2021) https:/doi.org/10.1111/febs.16066.

24. E. K. Perry, D. K. Newman, The transcription factors ActR and SoxR differentially affect the phenazine tolerance of Agrobacterium tumefaciens. *Mol Microbiol* **112**, 199–218 (2019).

25. T. Muth, *et al.*, JDet: Interactive calculation and visualization of function-related conservation patterns in multiple sequence alignments and structures. *Bioinformatics* **28**, 584–586 (2012).

26. I. G. Boneca, The role of peptidoglycan in pathogenesis. *Curr Opin Microbiol* **8**, 46–53 (2005).

27. R. E. Schaub, J. P. Dillard, The Pathogenic Neisseria Use a Streamlined Set of Peptidoglycan Degradation Proteins for Peptidoglycan Remodeling, Recycling, and Toxic Fragment Release. *Frontiers in Microbiology* **10** (2019).

28. R. S. Rosenthal, W. Nogami, B. T. Cookson, W. E. Goldman, W. J. Folkening, Major fragment of soluble peptidoglycan released from growing Bordetella pertussis is tracheal cytotoxin. *Infection and Immunity* **55**, 2117–2120 (1987).

29. S. Mattoo, J. D. Cherry, Molecular Pathogenesis, Epidemiology, and Clinical Manifestations of Respiratory Infections Due to Bordetella pertussis and Other Bordetella Subspecies. *Clin Microbiol Rev* **18**, 326–382 (2005).

30. Y. Dai, V. Pinedo, A. Y. Tang, F. Cava, E. Geisinger, A New Class of Cell Wall-Recycling l,d-Carboxypeptidase Determines β-Lactam Susceptibility and Morphogenesis in Acinetobacter baumannii. *mBio* **12**, e0278621 (2021).

31. B. W. Simpson, *et al.*, Acinetobacter baumannii Can Survive with an Outer Membrane Lacking Lipooligosaccharide Due to Structural Support from Elongasome Peptidoglycan Synthesis. *mBio* **12**, e0309921 (2021).

32. P. J. B. Brown, *et al.*, Polar growth in the Alphaproteobacterial order Rhizobiales. *Proceedings of the National Academy of Sciences of the United States of America* **109**, 1697–1701 (2012).

33. E. Krol, *et al.*, Tol-Pal System and Rgs Proteins Interact to Promote Unipolar Growth and Cell Division in Sinorhizobium meliloti. *mBio* **11**, e00306-20 (2020).

34. A. I. Weaver, *et al.*, Lytic transglycosylases mitigate periplasmic crowding by degrading soluble cell wall turnover products. *Elife* **11**, e73178 (2022).

35. M. W. Breedveld, K. J. Miller, Cyclic beta-glucans of members of the family Rhizobiaceae. *Microbiol Rev* **58**, 145–161 (1994).

36. S. Giacomucci, L. Alvarez, C. D. A. Rodrigues, F. Cava, C. Paradis-Bleau, Hydroxyl Radical Overproduction in the Envelope: an Achilles' Heel in Peptidoglycan Synthesis. *Microbiol Spectr* **10**, e0120321 (2022).

37. M. F. F. Arnold, *et al.*, Genome-Wide Sensitivity Analysis of the Microsymbiont Sinorhizobium meliloti to Symbiotically Important, Defensin-Like Host Peptides. *mBio* **8**, e01060-17 (2017).

592 38. T. H. Mauchline, *et al.*, Mapping the Sinorhizobium meliloti 1021 solute-binding protein-dependent transportome.
593 *Proceedings of the National Academy of Sciences* **103**, 17933–17938 (2006).

594 39. J. P. W. Young, *et al.*, The genome of Rhizobium leguminosarum has recognizable core and accessory components.
595 *Genome Biology* **7**, R34 (2006).

596 40. J. Prell, *et al.*, The PTSNtr system globally regulates ATP-dependent transporters in Rhizobium leguminosarum.
597 *Molecular Microbiology* **84**, 117–129 (2012).

598 41. V. Untiet, *et al.*, ABC transport is inactivated by the PTS(Ntr) under potassium limitation in Rhizobium leguminosarum
599 3841. *PLoS One* **8**, e64682 (2013).

600 42. G. Mulley, *et al.*, Mutation of GOGAT prevents pea bacteroid formation and N2 fixation by globally downregulating
601 transport of organic nitrogen sources. *Mol Microbiol* **80**, 149–167 (2011).

602 43. G. Cheng, R. Karunakaran, A. K. East, O. Munoz-Azcarate, P. S. Poole, Glutathione affects the transport activity of
603 Rhizobium leguminosarum 3841 and is essential for efficient nodulation. *FEMS Microbiol Lett* **364** (2017).

604 44. J. Hartl, *et al.*, Untargeted metabolomics links glutathione to bacterial cell cycle progression. *Nat Metab* **2**, 153–166
605 (2020).

606 45. E. R. Morton, C. Fuqua, Laboratory Maintenance of Agrobacterium. *Current Protocols in Microbiology* **73**, 141–151
607 (2012).

608 46. E. R. Morton, C. Fuqua, Genetic manipulation of Agrobacterium. *Current Protocols in Microbiology*, 1–15 (2012).

609 47. L. Alvarez, S. B. Hernandez, M. A. De Pedro, F. Cava, "Ultra-Sensitive, High-Resolution Liquid Chromatography
610 Methods for the High-Throughput Quantitative Analysis of Bacterial Cell Wall Chemistry and Structure" in *Bacterial Cell*
611 *Wall Homeostasis: Methods and Protocols*, (2016).

612 48. F. Cava, M. A. De Pedro, H. Lam, B. M. Davis, M. K. Waldor, Distinct pathways for modification of the bacterial cell wall
613 by non-canonical D-amino acids. *EMBO Journal* **30**, 3442–3453 (2011).

614 49. M. N. Price, *et al.*, Mutant phenotypes for thousands of bacterial genes of unknown function. *Nature* **557**, 503–509
615 (2018).

616 50. J. Huerta-Cepas, *et al.*, eggNOG 5.0: a hierarchical, functionally and phylogenetically annotated orthology resource
617 based on 5090 organisms and 2502 viruses. *Nucleic Acids Research* **47**, D309–D314 (2019).

618 51. R. C. Edgar, MUSCLE: multiple sequence alignment with high accuracy and high throughput. *Nucleic Acids Research*
619 **32**, 1792–1797 (2004).

620 52. G. E. Crooks, G. Hon, J.-M. Chandonia, S. E. Brenner, WebLogo: a sequence logo generator. *Genome Res* **14**, 1188–
621 1190 (2004).

622 53. E. V. Kriventseva, *et al.*, OrthoDB v10: sampling the diversity of animal, plant, fungal, protist, bacterial and viral
623 genomes for evolutionary and functional annotations of orthologs. *Nucleic Acids Research* **47**, D807–D811 (2019).

624 54. I. Letunic, P. Bork, Interactive Tree Of Life (iTOL) v5: an online tool for phylogenetic tree display and annotation. *Nucleic*
625 *Acids Research* **49**, W293–W296 (2021).

626 55. M. C. Chao, *et al.*, High-resolution definition of the Vibrio cholerae essential gene set with hidden Markov model-based
627 analyses of transposon-insertion sequencing data. *Nucleic Acids Research* **41**, 9033–9048 (2013).

628 56. S. L. Chiang, E. J. Rubin, Construction of a mariner-based transposon for epitope-tagging and genomic targeting. *Gene*
629 **296**, 179–185 (2002).

630 57. J. R. Pritchard, *et al.*, ARTIST: High-Resolution Genome-Wide Assessment of Fitness Using Transposon-Insertion
631 Sequencing. *PLoS Genetics* **10** (2014).

632

Figures

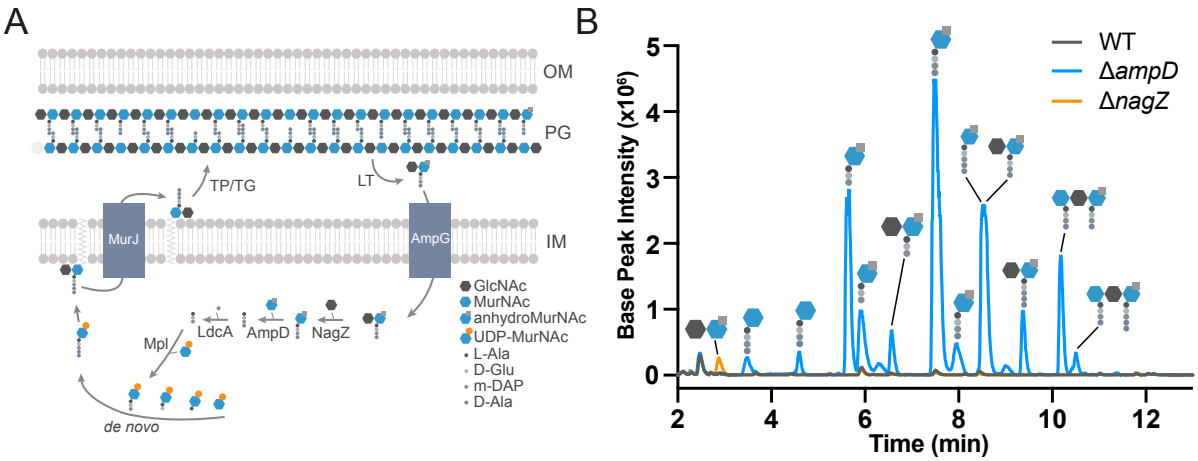

Figure 1. *A. tumefaciens* recycles muropeptides. (A). Schematic diagram of PG recycling pathway in *E. coli*. TP, transpeptidase; TG, transglycosylase; LT, lytic transglycosylase; OM, outer membrane; PG, peptidoglycan; IM, inner membrane. (B). Soluble PG fragments that accumulate in the cytoplasm of *A. tumefaciens* WT, Δ*ampD* and Δ*nagZ* strains detected using LC-MS.

641

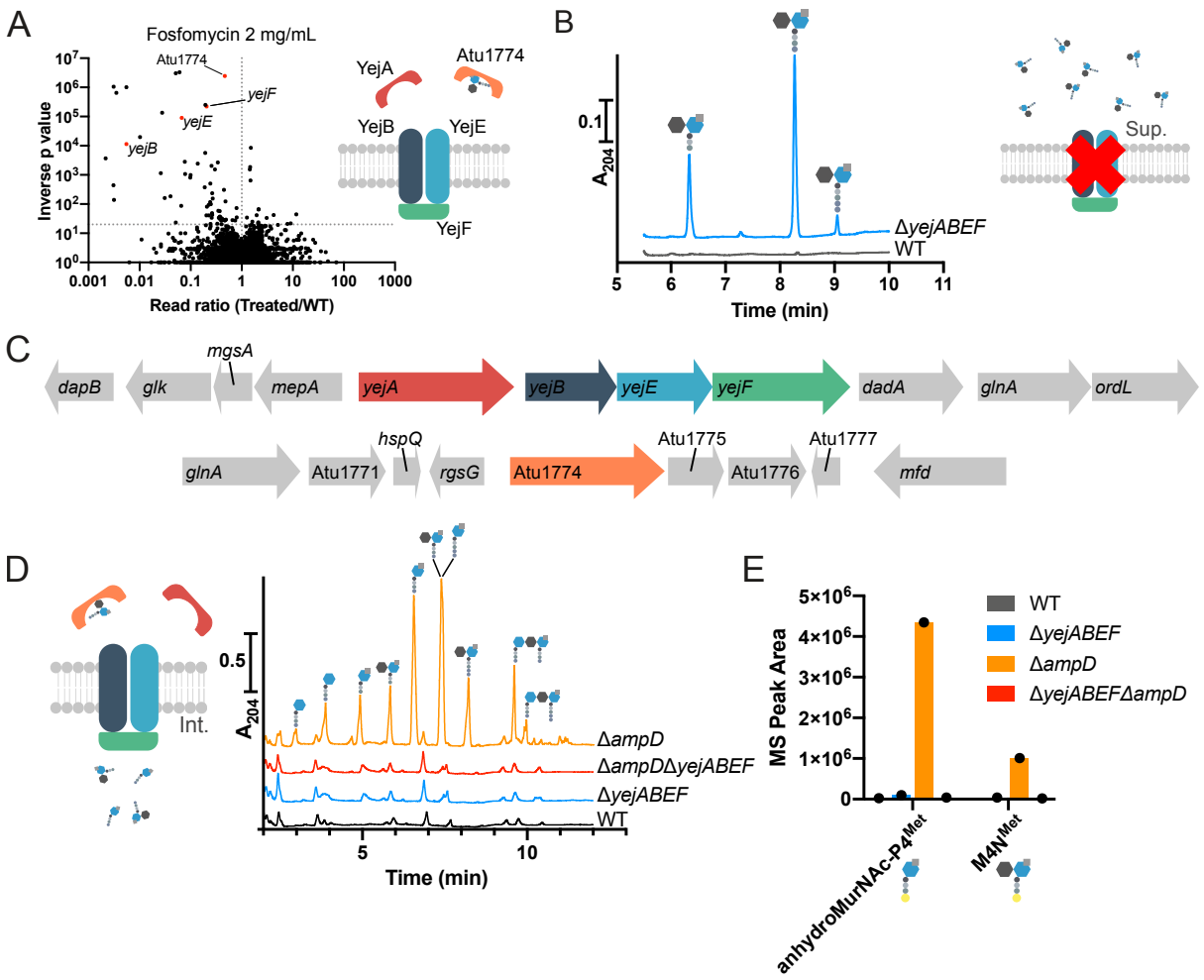

642

643 Figure 2. YejBEF is the PG recycling transporter in *A. tumefaciens*. (A). Volcano plot
644 showing the ratio of Transposon sequencing (Tn-Seq) reads mapped to genes in the
645 *A. tumefaciens* WT strain treated with 2 mg/mL Fosfomycin compared to control,
646 plotted against inverse p-value. Genes corresponding to *yejBEF* and Atu1774 are
647 highlighted in red. (B). UPLC chromatogram showing levels of anhydromuropeptides
648 released into the supernatants by *A. tumefaciens* WT and Δ*yejABEF* strains (C).
649 Genomic context of *yejABEF* and Atu1774. (D). Soluble PG fragments that
650 accumulate in *A. tumefaciens* WT, Δ*yejABEF*, Δ*ampD* and Δ*yejABEF*Δ*ampD* strains
651 detected using UPLC.

652

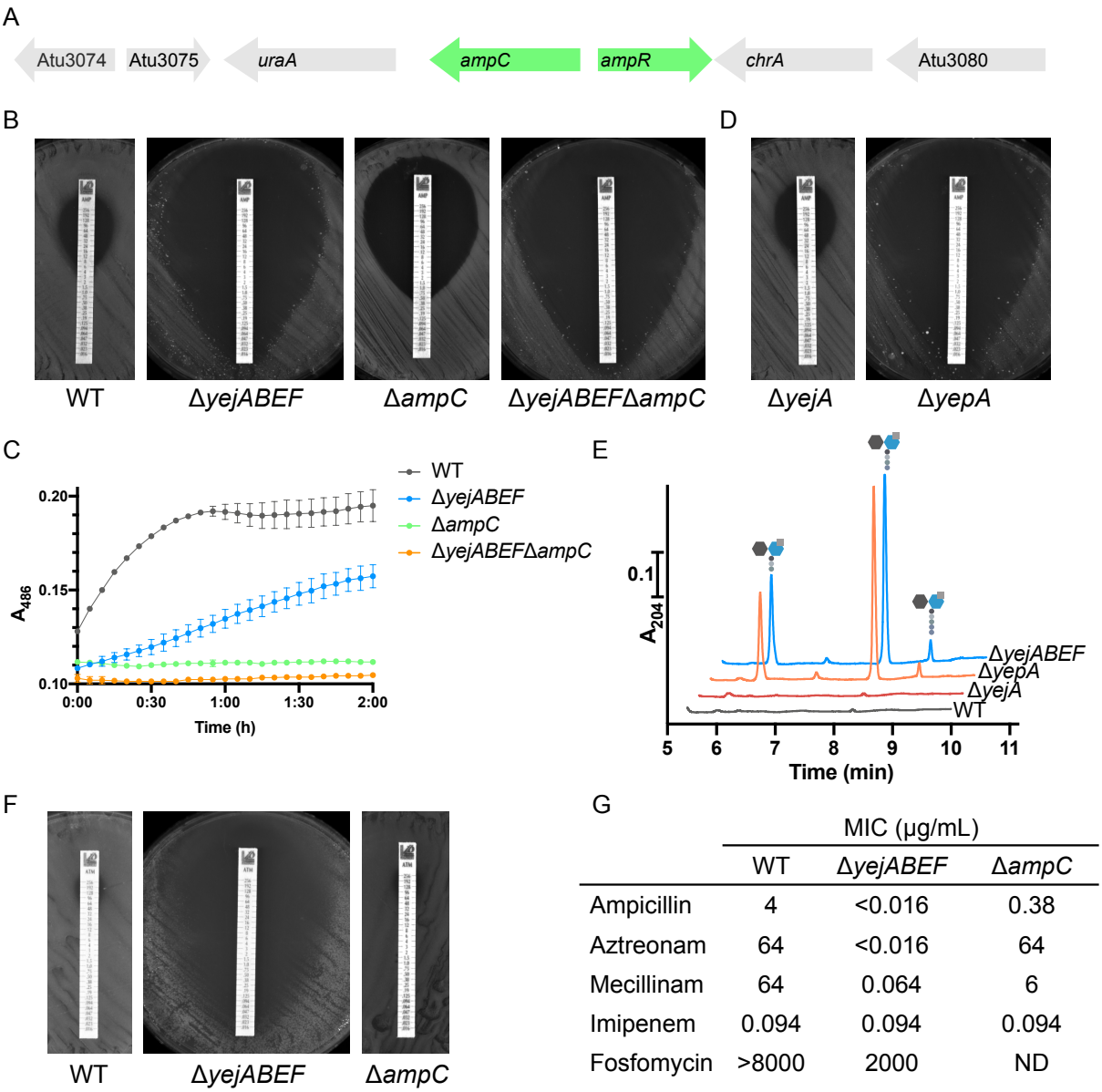

G

	MIC (μg/mL)		
	WT	Δ*yejABEF*	Δ*ampC*
Ampicillin	4	<0.016	0.38
Aztreonam	64	<0.016	64
Mecillinam	64	0.064	6
Imipenem	0.094	0.094	0.094
Fosfomycin	>8000	2000	ND

Figure 3. Δ*yejABEF* is hypersensitive to Ampicillin, in a manner only partly dependent on the β-lactamase AmpC. (A). Genomic context of the AmpC β-lactamase in A. tumefaciens, showing proximity to canonical AmpR repressor. (B). Comparison of Amp resistance of A. tumefaciens WT, Δ*yejABEF*, Δ*ampC* and Δ*yejABEF*Δ*ampC* strains by growth on LB plates with Ampicillin MIC test strips. (C). Hydrolysis of nitrocefin by lysates of *A. tumefaciens* WT, Δ*yejABEF*, Δ*ampC* and Δ*yejABEF*Δ*ampC* strains, measured by following A_{486}. (D). Comparison of Amp resistance of *A. tumefaciens* Δ*yejA* and Δ*yepA* strains. (E). Accumulation of

662 muropeptides in the supernatants of *A. tumefaciens* WT, Δ*yepA*, Δ*yejA* and
663 Δ*yejABEF* strains, measured by UPLC. (F). Comparison of Aztreonam resistance of
664 A. tumefaciens WT, Δ*yejABEF* and Δ*ampC* strains by growth on LB plates with
665 Aztreonam MIC test strips. (G). Minimal inhibitory concentration (MIC) values of A.
666 tumefaciens WT, Δ*yejABEF* and Δ*ampC* to β-lactams Ampicillin, Aztreonam,
667 Mecillinam, Imipenem, and MurA-inhibitor Fosfomycin.

668

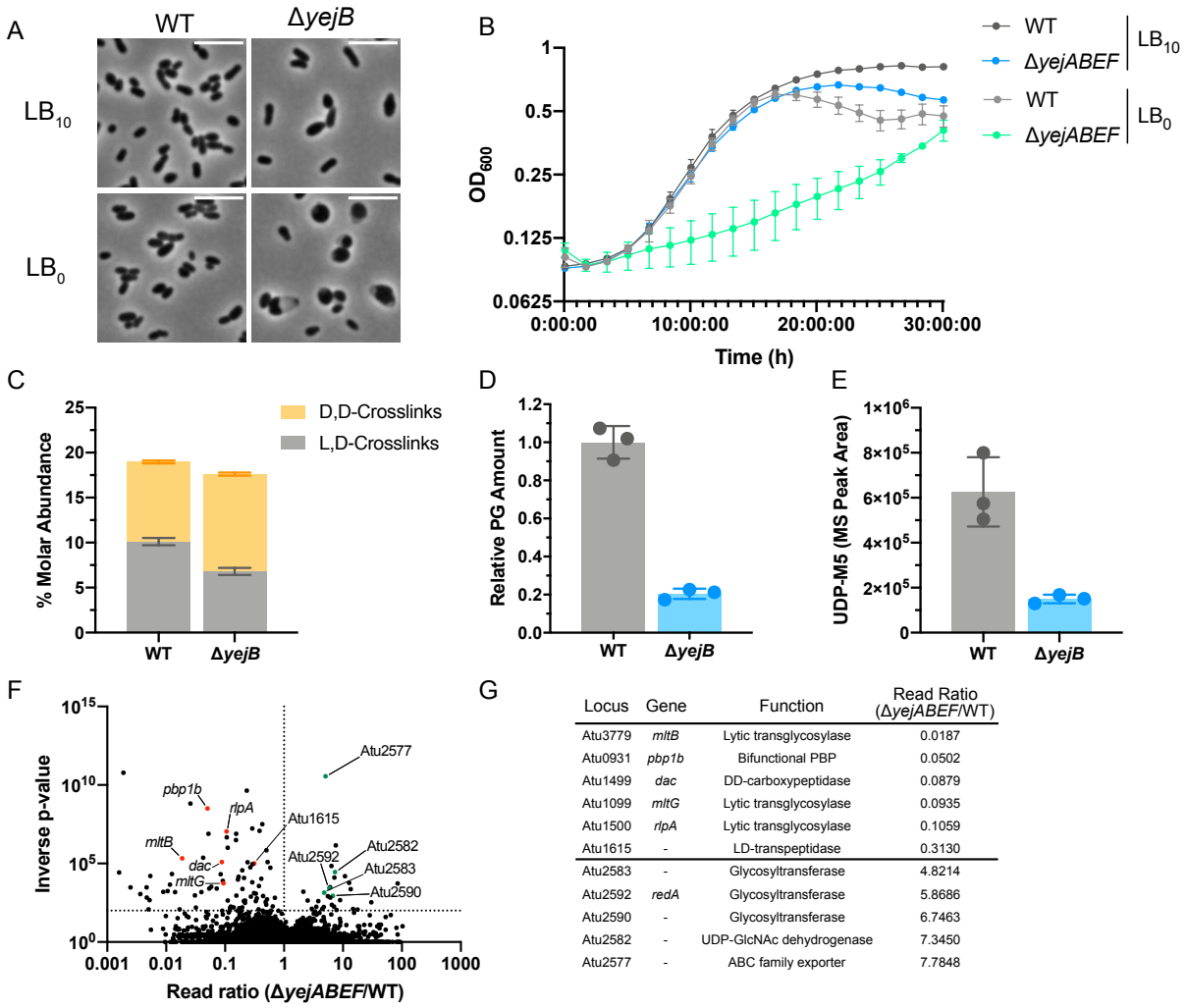

Locus	Gene	Function	Read Ratio (ΔyejABEF/WT)
Atu3779	*mltB*	Lytic transglycosylase	0.0187
Atu0931	*pbp1b*	Bifunctional PBP	0.0502
Atu1499	*dac*	DD-carboxypeptidase	0.0879
Atu1099	*mltG*	Lytic transglycosylase	0.0935
Atu1500	*rlpA*	Lytic transglycosylase	0.1059
Atu1615	-	LD-transpeptidase	0.3130
Atu2583	-	Glycosyltransferase	4.8214
Atu2592	*redA*	Glycosyltransferase	5.8686
Atu2590	-	Glycosyltransferase	6.7463
Atu2582	-	UDP-GlcNAc dehydrogenase	7.3450
Atu2577	-	ABC family exporter	7.7848

Figure 4. PG recycling is required for cell wall integrity in *A. tumefaciens*. (A-E). Phenotypic analysis of *A. tumefaciens* WT and Δ*yejABEF* strains. (A). Phase contrast microscopy of WT and Δ*yejB* cells grown on LB_{10} and LB_0. (B). Growth curves of WT and Δ*yejABEF* on LB_{10} and LB_0. (C). Molar abundance of DD- and LD-crosslinks in cell walls determined by UPLC analysis of WT and Δ*yejB* PG. (D). Relative PG amounts determined by total area under UPLC chromatograms of WT and Δ*yejB* PG. (E). LC-MS quantification of primary soluble PG precursor UDP-M5 in WT and Δ*yejB*. (F). Volcano plot showing the ratio of Tn-Seq reads mapped to genes in the *A. tumefaciens* Δ*yejABEF* strain compared to WT as control. Selected

680 synthetically detrimental (red) and synthetically beneficial (green) hits are

681 highlighted. (G). Table listing selected synthetically detrimental or beneficial hits in

682 Δ*yejABEF* Tn-Seq with annotations.

683

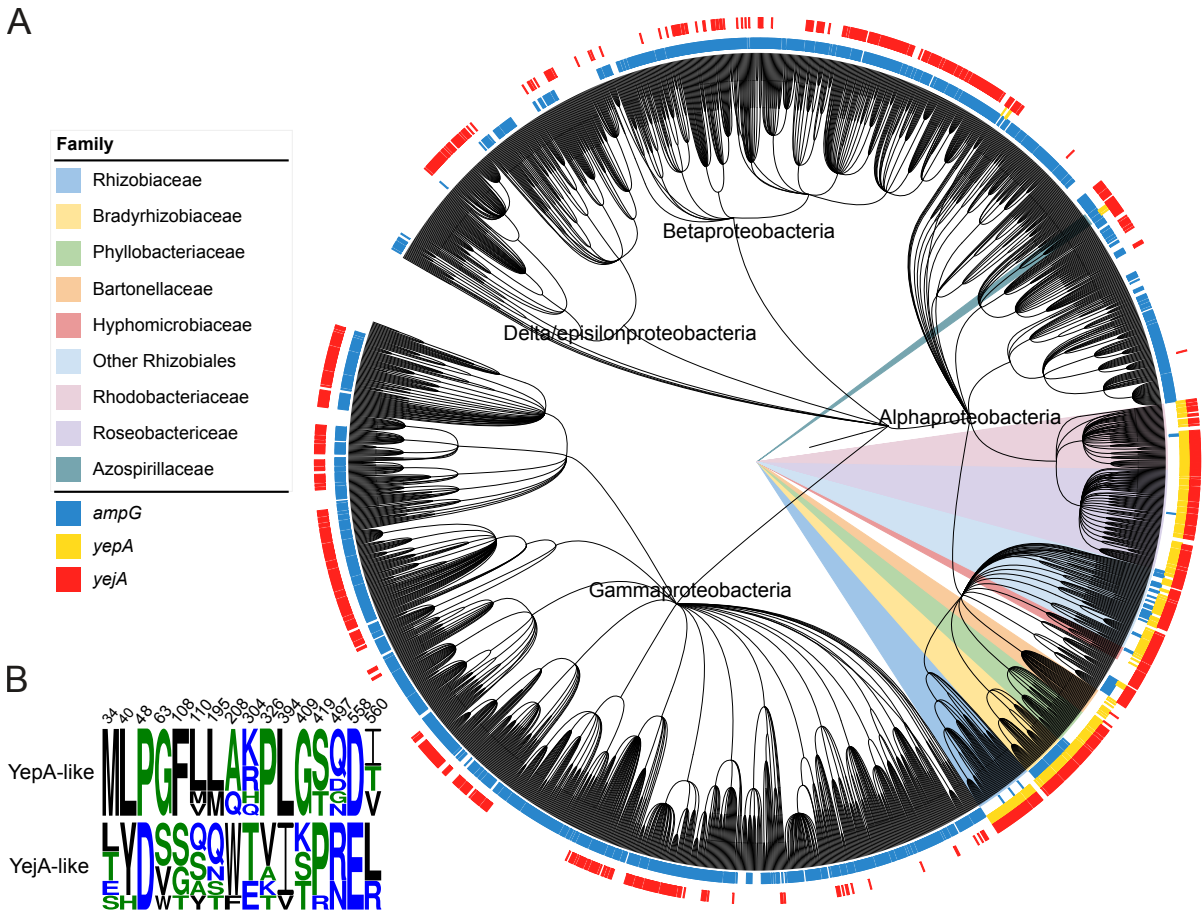

Figure 5. YejABEF is widespread in the proteobacteria, but YepA is only present in the Alphaproteobacteria. (A). Phylogenetic tree showing distribution of *ampG*, *yejA* and *yepA* in the proteobacteria. (B). Molecular fingerprint residues of YepA used to differentiate between YejA and YepA.

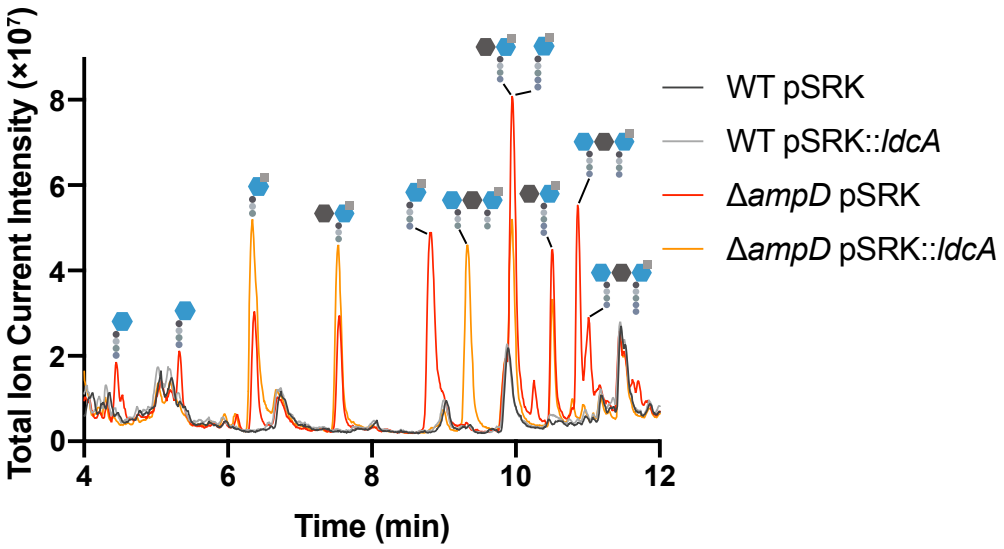

690

691 Supplementary Figure 1. Detection of accumulating muropeptide species in *A.*

692 *tumefaciens* WT and Δ*ampD* strains containing expression vector with or without *E.*

693 *coli ldcA* using LC-MS.

694

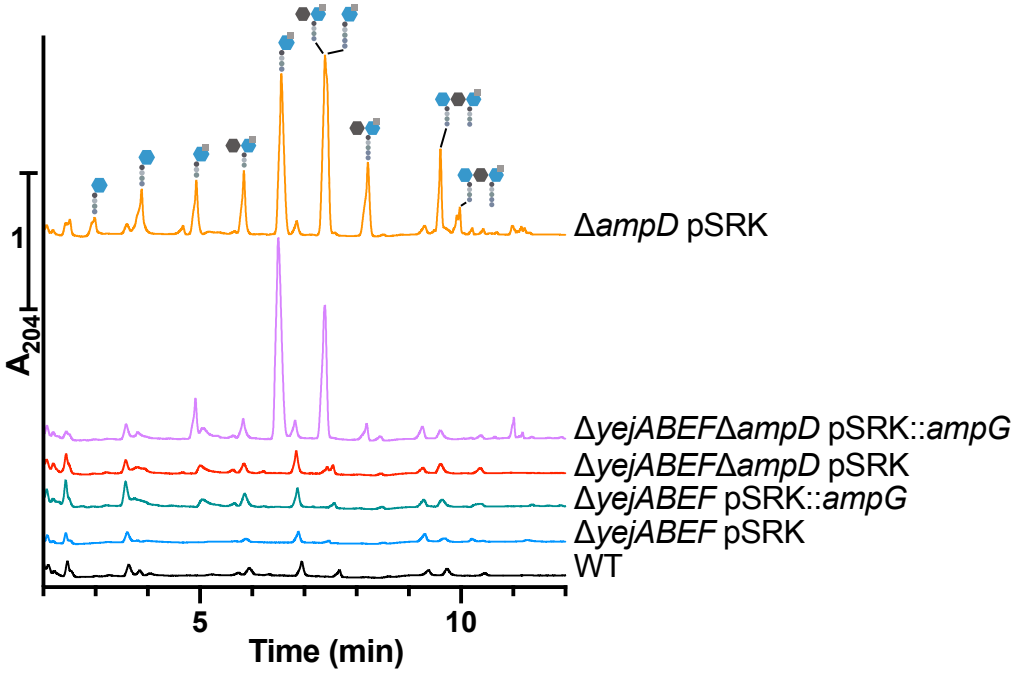

Supplementary Figure 2. Detection of accumulating muropeptide species in A. tumefaciens WT, Δ*ampD*, Δ*yejABEF* and Δ*yejABEF*Δ*ampD* containing expression vector with or without *E. coli ampG* using UPLC.

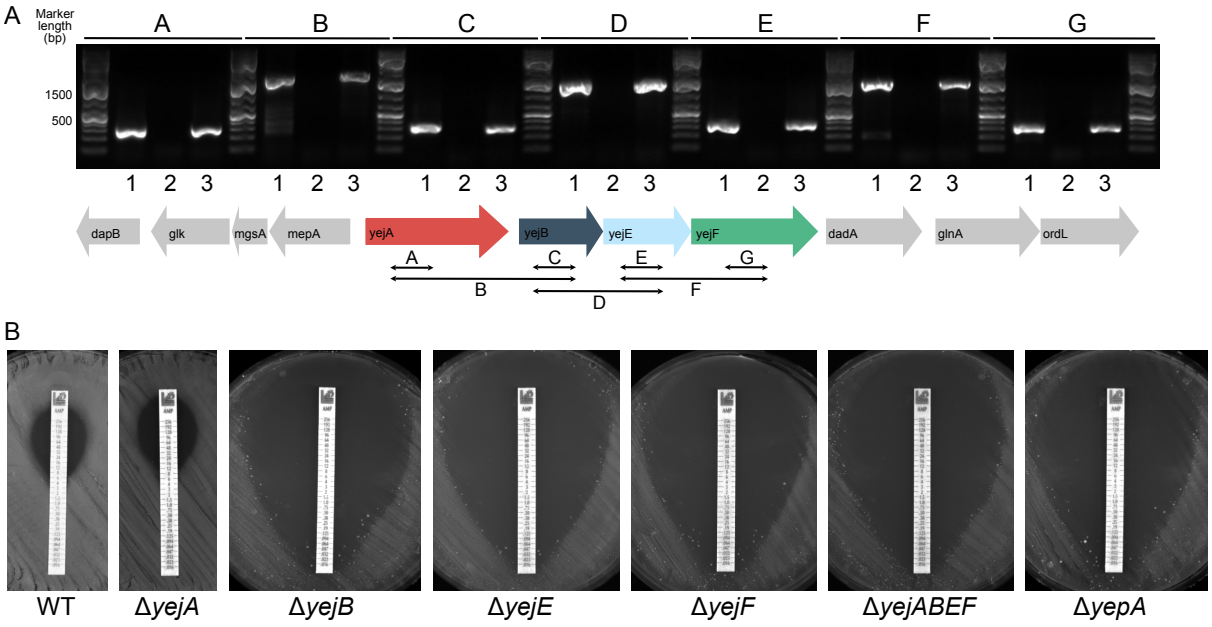

Supplementary Figure 3. *yejABEF* genes are co-transcribed, but *yejA* is not involved in PG recycling. (A). PCR amplification using as template: 1. gDNA; 2. RT reaction without added RT; 3. cDNA. Inter- and intragenic regions amplified are indicated below. (B). Ampicillin MIC test strips of *A. tumefaciens* WT, Δ*yejA*, Δ*yejB*, Δ*yejE*, Δ*yejF*, Δ*yejABEF* and Δ*yepA*.

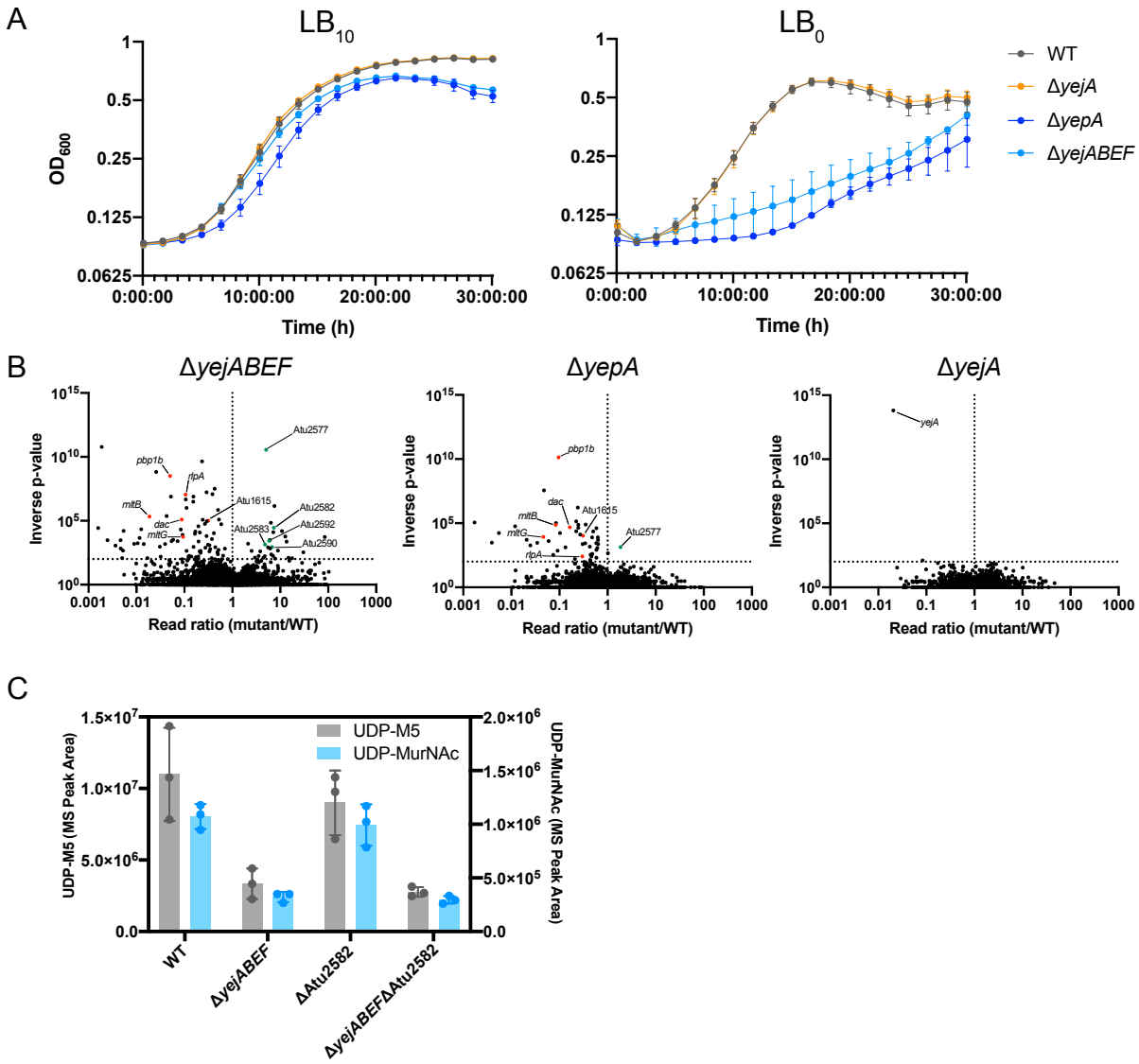

Supplementary Figure 4. PG recycling is required for cell wall integrity in *A. tumefaciens* (cont.). (A). Growth curves of *A. tumefaciens* WT, Δ*yejA*, Δ*yepA* and Δ*yejABEF* strains on LB_{10} and LB_0. (B). Volcano plot showing the ratio of Tn-Seq reads mapped to genes in the *A. tumefaciens* Δ*yejABEF*, Δ*yepA* and Δ*yejA* strains compared to WT as control. Selected synthetically detrimental (red) and synthetically beneficial (green) hits are highlighted. (C) Quantification of PG precursors UDP-M5 and UDP-MurNAc in *A. tumefaciens* WT, Δ*yejABEF*, ΔAtu2582 and Δ*yejABEF*ΔAtu2582 strains using LC-MS.